PILOT-SYMBOL ASSISTED CARRIER SYNCHRONIZATION: CRAMER-RAO BOUND AND SYNCHRONIZER PERFORMANCE

N. Noels, H. Steendam and M. Moeneclaey
TELIN department, Ghent University, St-Pietersnieuwstraat 41, B-9000 GENT, BELGIUM
Tel: (+32) 9 264 34 26, Fax: (+32) 9 264 42 95
Mailto: {nnoels, hs, mm} @telin.UGent.be

***Abstract* - This contribution considers the joint estimation of the carrier phase and the frequency offset from a noisy linearly modulated burst signal containing random data symbols (DS) as well as known pilot symbols (PS). The corresponding Cramer-Rao lower bound (CRB) is derived. This bound indicates that it is potentially more accurate to estimate carrier phase and frequency from such a '*hybrid*' burst than from a burst without PS or from the limited number of PS only. The new bound is compared with the performance of new and existing carrier synchronizers. We present the iterative soft-Decision-Directed (sDD) estimator with combined data-aided/non-data-aided (DA/NDA) initialization, which performs closely to the CRB, and provides a large improvement over the classical NDA estimator at low and moderate signal-to-noise ratio (SNR).**

I. INTRODUCTION

In burst digital transmission with coherent detection, the recovery of the carrier phase and frequency offset is a key aspect. We assume that phase coherence over successive bursts cannot be maintained, so that the carrier phase and frequency offset have to be recovered on a burst-by-burst basis.

Most classical synchronizers belong to one of the following types: *Data-Aided* (DA) synchronization algorithms use known pilot symbols (PS), while N*on-Data-Aided* (NDA) and *Decision-Directed* (DD) estimators operate on modulated data symbols (DS). DD estimators are similar to DA estimators, but use, instead of PS, hard or soft decisions regarding the DS, that are provided by the detector; NDA estimators apply a non-linearity to the received signal to remove the data modulation.

Assuming that the parameter estimate is unbiased, the variance of the estimation error is often used as a performance measure. The Cramer-Rao lower bound (CRB) is a fundamental lower bound on the variance of any unbiased estimate [1], and is also known to be asymptotically achievable for a large enough number of observations, under mild regularity conditions. The $CRB_{PS}(N_p)$ for phase and/or frequency estimation from N_p known PS has been derived in [2-3]. The $CRB_{DS}(N_d)$ related to joint carrier phase and frequency estimation from N_d random DS has been addressed in [4-7]. In order to avoid the computational complexity related to the true CRB_{DS}, a modified CRB (MCRB) has been derived in [8,9]. The MCRB is much easier to evaluate than the CRB, but is in general looser (i.e. lower) than the true CRB, especially at lower signal-to-noise ratio (SNR). In [10], the high-SNR limit of the CRB_{DS} has been obtained analytically, and has been shown to coincide with the MCRB.

Except for very high signal-to-noise ratio (SNR) and/or very large bursts, accurate estimation of large frequency offsets is far from trivial.

- It is well known that many frequency algorithms do not work properly at lower values of E_s/N_0 because of the so-called *threshold phenomenon* [2]. This consists of the occurrence of large, spurious frequency errors when the SNR drops below a certain threshold, and results in a very high frequency error variance that steeply diverges from the CRB at SNR below threshold. Estimators that operate on short bursts and/or use NDA techniques, typically have a high SNR threshold.
- On the other hand, from [2-7] we know that the CRB for frequency estimation typically decreases with the third power of the number of available samples. As efficient transmission demands that the number of PS in a burst is kept small as compared to the overall burst length, this implies that NDA and DD estimators (using DS) are potentially more accurate than DA estimators (using the PS only).

Hence, in many practical situations frequency estimators that use *random DS only* have a high SNR threshold but a low estimation error bound, whereas frequency estimators that use *known PS only* have a low threshold but a high estimation error bound. In [11], it has been shown that a frequency estimator that utilizes *both PS and DS* may provide the combined

advantages of DA estimators and NDA estimators, and allow more accurate synchronization at lower SNR.

It is obvious that phase estimation may also benefit from the simultaneous use of PS and DS. The PS allow to resolve the phase ambiguity caused by the rotation symmetry of the constellation, while the DS guarantee a good performance at high SNR (from [2-7] we know that the CRB for phase estimation is inversely proportional to the number of available samples).

This contribution further examines joint phase and frequency estimation from the observation of a burst that contains N_p pilot-symbols as well as N_d data symbols. In Section III, we derive the corresponding true $CRB_{PS\text{-}DS}(N_p,N_d)$, which can be viewed as a generalization of both CRB_{PS} and CRB_{DS}. Numerical results are reported for a QPSK constellation, indicating that it is potentially more accurate to estimate carrier phase and frequency from a hybrid burst than from a burst without PS or from a limited number of PS only. Comparing, in Section IV, the true CRB to the performance of the estimation algorithm from [11], that uses both PS and DS, it is concluded that more efficient 'hybrid' algorithms may exist that perform more closely to the new $CRB_{PS\text{-}DS}$. We propose some new algorithms, including an iterative soft-DD (sDD) estimator with combined DA/NDA initialization that yields a close agreement between the simulated performance and the $CRB_{PS\text{-}DS}$. Section V concludes this paper.

II. Problem Formulation

Consider the following observation model

$$r_k = a_k e^{j\theta_k} + w_k, \quad k \in I = \{-K, -K+1, \ldots, K\} \quad (1)$$

In (1), $\{a_k: k \in I\}$ is a sequence of $L = 2K+1$ transmitted PSK, QAM or PAM symbols. For ease of exposition, we are assuming that L is an odd integer. The case of even L needs only slight modifications. We assume a_k belongs to the symbol alphabet $\{\alpha_0, \alpha_1, ..., \alpha_{M-1}\}$, with M denoting the number of constellation points and $E[|a_k|^2]=1$. The symbol a_k denotes a known PS for k belonging to the set of indices $I_p=\{k_0, k_1, \ldots, k_{Np-1}\} \subseteq I$, where N_p denotes the number of PS. For $k \in I_d=\{I \setminus I_p\}$, a_k denotes an unknown DS. The N_d (=L-N_p) DS are assumed to be statistically independent and uniformly distributed over the constellation, i.e., the transmitted DS can take any value from the symbol alphabet with equal probability. The sequence $\{w_k: k \in I\}$ consists of zero-mean complex Gaussian noise variables, with independent real and imaginary parts each having a variance of $N_0/2E_s$. The quantities E_s and N_0 denote the symbol energy and the noise power spectral density ($SNR = E_s/N_0$), respectively. The quantity θ_k is defined as $(\theta + 2\pi kFT)$, where θ represents the carrier phase at k = 0, F is the frequency offset and T is the symbol duration. Both θ and F are unknown but deterministic parameters. The observation $\{r_k\}$ consists of the matched filter output samples taken at the correct timing instants kT. Note that we assume $|FT| << 1$, so that the useful signal reduction and the ISI caused by a nonzero frequency offset at the input of the matched filter can be safely ignored. It has been show in [7] that at practical SNR values the simplified discrete-time observation (1) yields essentially the same CRB as the correct continuous-time observation model.

Let us denote by $p(\mathbf{r};\mathbf{u})$ the probability density function (pdf) of the observation vector $\mathbf{r}$, where $\mathbf{u}$ is an unkown deterministic vector parameter. Suppose one is able to produce from $\mathbf{r}$ an unbiased estimate $\hat{\mathbf{u}}$ of the parameter $\mathbf{u}$. Then the estimation error covariance matrix $R_{\hat{\mathbf{u}}-\mathbf{u}} = E[(\hat{\mathbf{u}}-\mathbf{u})(\hat{\mathbf{u}}-\mathbf{u})^T]$ satisfies

$$R_{\hat{\mathbf{u}}-\mathbf{u}} - J^{-1}(\mathbf{u}) \geq 0 \qquad (\textit{positive semi definite}) \quad (2)$$

where $J(\mathbf{u})$ is the Fisher information matrix (FIM). The (i,j)-th element of $\mathbf{J}(\mathbf{u})$ is given by

$$\mathbf{J}_{i,j}(\mathbf{u}) = E_{\mathbf{r}}\left[\frac{\partial}{\partial u_i}\ln(p(\mathbf{r};\mathbf{u}))\frac{\partial}{\partial u_j}\ln(p(\mathbf{r};\mathbf{u}))\right] \quad (3)$$

Note that $\mathbf{J}(\mathbf{u})$ is a symmetrical matrix. When the element $\mathbf{J}_{ij}(\mathbf{u}) = 0$, the parameters u_i and u_j are said to be *decoupled*. The expectation $E_{\mathbf{r}}[.]$ in (3) is with respect to $p(\mathbf{r};\mathbf{u})$. The probability density $p(\mathbf{r};\mathbf{u})$ of **r,** corresponding to a given value of $\mathbf{u}$, is called the *likelihood function* of $\mathbf{u}$, $\ln(p(\mathbf{r};\mathbf{u}))$ is the *log-likelihood function* of $\mathbf{u}$. When the observation $\mathbf{r}$ depends not only on the parameter $\mathbf{u}$ to be estimated but also on a nuisance vector parameter $\mathbf{v}$, the likelihood function of $\mathbf{u}$ is obtained by averaging the likelihood function $p(\mathbf{r}|\mathbf{v};\mathbf{u})$ of the vector $(\mathbf{u},\mathbf{v})$ over the a priori distribution of the nuisance parameter: $p(\mathbf{r};\mathbf{u}) = E_{\mathbf{v}}[p(\mathbf{r} \mid \mathbf{v};\mathbf{u})]$. We refer to $p(\mathbf{r}|\mathbf{v};\mathbf{u})$ as the joint likelihood function, as $p(\mathbf{r}|\mathbf{v};\mathbf{u})$ is relevant to the joint ML estimation of $\mathbf{u}$ and $\mathbf{v}$.

Considering the joint estimation of the carrier phase θ and frequency offset F from the observation vector $\mathbf{r} = \{r_k\}$ from (1), we take $\mathbf{u} = (u_1,u_2) = (\theta,F)$. The nuisance parameter vector $\mathbf{v} = \{a_k: k \in I_d\}$ consists of the unknown DS. Within a factor not depending on F, θ and $\mathbf{a}$, the joint likelihood function $p(\mathbf{r}|\mathbf{a};F,\theta)$ is given by

$$p(\mathbf{r} \mid \mathbf{a}; F, \theta) = \prod_{k \in I} F(a_k, \tilde{r}_k) \quad (4)$$

where

$$F(a_k, \tilde{r}_k) = e^{\frac{E_s}{N_0}\left(2\,\mathrm{Re}(a_k^* \tilde{r}_k) - |a_k|^2\right)} \quad (5)$$

and $\tilde{r}_k = r_k e^{-j(2\pi kFT+\theta)}$. Averaging (4) over the data symbols yields the likelihood function $p(\mathbf{r};F,\theta)$. For the log-likelihood function $\ln(p(\mathbf{r};F,\theta))$ we obtain, within a term that does not depend on (F,θ)

$$\ln p(\mathbf{r};F,\theta) = 2\frac{E_s}{N_0}\mathrm{Re}\left(e^{-j\theta}\sum_{k\in I_p} a_k^*\tilde{r}_k \right) + \sum_{l\in I_d}\ln I(\tilde{r}_l) \quad (6)$$

where

$$I(\tilde{r}_k) = \sum_{i=0}^{M-1} F(\alpha_i, \tilde{r}_k) \quad (7)$$

and $\{\alpha_0, \alpha_1, ..., \alpha_{M-1}\}$ denotes the set of constellation points.

It follows from (2) that the error variance regarding the estimation of θ and F is lower bounded by the Cramer-Rao Bound (CRB):

$$E_r[(\hat{\theta}-\theta)^2] \geq CRB_\theta^{PS-DS} = \left(\mathbf{J}^{-1}_{(\theta,F)}\right)_{11} \quad (8)$$

$$E_r[(\hat{F}-F)^2] \geq CRB_{FT}^{PS-DS} = \left(\mathbf{J}^{-1}_{(\theta,F)}\right)_{22} \quad (9)$$

where $\mathbf{J}^{-1}$ denotes the inverse of the FIM. Similarly, (2) yields a lower bound on the variance of the estimation error on the instantaneous phase:

$$E_r[(\hat{\theta}_k-\theta_k)^2] \geq CRB_{\theta_k}^{PS-DS} = \left(\mathbf{J}^{-1}_{(\theta,F)}\right)_{11} + 4\pi kT\left(\mathbf{J}^{-1}_{(\theta,F)}\right)_{12} + 4(\pi kT)^2\left(\mathbf{J}^{-1}_{(\theta,F)}\right)_{22} \quad (10)$$

As the evaluation of the various expectations in $\mathbf{J}(\theta,F)$ and $p(\mathbf{r}|\theta,F)$ is quite tedious a simpler lower bound, called modified CRB (MCRB), has been derived in [8,9], i.e., $E[(\hat{x}-x)^2] \geq CRB_x^{PS-DS} \geq MCRB_x^{PS-DS}$, where $MCRB_x$ is defined as CRB_x in (8-10) but with the FIM $\mathbf{J}(\theta,F)$ replaced with the modified FIM (MFIM) $\mathbf{J}_M(\theta,F)$ given by

$$\mathbf{J}_M = \frac{2E_s}{N_0} L\begin{bmatrix} 1 & 0 \\ 0 & \pi^2T^2(L^2-1)/3 \end{bmatrix} \quad (11)$$

III. Evaluation Of The CRB

Partial differentiation of the log-likelihood function (6) with respect to the carrier phase θ and the frequency offset F yields

$$\frac{\partial}{\partial\theta}\ln p(\mathbf{r};F,\theta) = 2\frac{E_s}{N_0}\left(\sum_{k\in I_p}\mathrm{Im}(a_k^*\tilde{r}_k) + \sum_{l\in I_d} M(\tilde{r}_l) \right) \quad (12)$$

$$\frac{\partial}{\partial F}\ln p(\mathbf{r};F,\theta) = 4\pi T\frac{E_s}{N_0}\left(\sum_{k\in I_p} k\,\mathrm{Im}(a_k^*\tilde{r}_k) + \sum_{l\in I_d} lM(\tilde{r}_l) \right) \quad (13)$$

where

$$M(\tilde{r}_k) = \sum_{i=0}^{M-1} F(\alpha_i,\tilde{r}_k)\mathrm{Im}(\alpha_i^*\tilde{r}_k)/I(\tilde{r}_k) \quad (14)$$

F(.,.) and I(.) are defined as in (5) and (7) respectively and $\{\alpha_0, \alpha_1, ..., \alpha_{M-1}\}$ denotes the set of constellation points. Substituting (12) and (13) into (3) yields

$$\mathbf{J}^{PS-DS} = \frac{2E_s}{N_0}\begin{bmatrix} \sum_{k\in I}\beta_k & 2\pi T\sum_{k\in I} k\beta_k \\ 2\pi T\sum_{k\in I} k\beta_k & (2\pi T)^2\sum_{k\in I} k^2\beta_k \end{bmatrix} = J_{11}\begin{bmatrix} 1 & 2\pi Tk_G \\ 2\pi Tk_G & (2\pi T)^2(k_G^2+\sigma_G^2) \end{bmatrix} \quad (15)$$

where

$$\beta_k = \begin{cases} |a_k|^2, & k\in I_p \\ \frac{2E_s}{N_0}E_r\left[M(r)^2\right], & k\in I_d \end{cases} \quad (16)$$

and

$$k_G = \frac{\sum_I k\beta_k}{\sum_I \beta_k} \qquad \sigma_G^2 = \frac{\sum_I (k-k_G)^2\beta_k}{\sum_I \beta_k} \quad (17)$$

In (16), $E_r[.]$ denotes the average over $r = a+n$, where a is a random variable that takes any value from the symbol alphabet with equal probability and n is complex zero-mean Gaussian noise with variance equal to N_0/E_s. The quantity k_G can be interpreted as the center of gravity of the sequence $\{\beta_k\}$. We obtain $J_{12}^{PS-DS} \neq 0$, unless $k_G = 0$, which is achieved if both PS and DS are each located symmetrically about zero, and the PS satisfy $|a_k|=|a_{-k}|$. For $k_G \neq 0$, the parameters θ and F are coupled, meaning that the inaccuracy in the carrier phase estimate has an impact on the frequency offset estimation and vice versa. In general, k_G is a function of the SNR. For very low SNR, k_G converges to the center of gravity of the pilot sequence. For an M-PSK constellation, the high-SNR limit of k_G equals 0, which implies that θ and F are always decoupled at high SNR. For M-PAM and M-QAM constellations the high-SNR limit of k_G depends on the particular pilot sequences that was selected and on the specific position of the PS in the burst. However, for $L >> N_p$ we can assume k_G to be approximately zero. Note that the FIM does not depend on θ or F. Substituting (15) into (8-10) we obtain

$$E[(\hat{\theta}-\theta)^2] \geq CRB_\theta^{PS-DS} = \frac{1}{J_{11}}\left(1+\frac{k_G^2}{\sigma_G^2}\right) \quad (18)$$

$$E[(\hat{FT}-FT)^2] \geq CRB_{FT}^{PS-DS} = \frac{1}{4\pi^2\sigma_G^2 J_{11}} \quad (19)$$

$$E[(\hat{\theta}_k-\theta_k)^2] \geq CRB_{\theta_k}^{PS-DS} = \frac{1}{J_{11}}\left(1+\frac{(k-k_G)^2}{\sigma_G^2}\right) \quad (20)$$

The lower bound on $E[(\hat{\theta}_k-\theta_k)^2]$ from (20) is *quadratic* in k. Its *minimum* value is achieved at $k = k_G$ and is equal to $1/J_{11}$, which is the CRB for the estimation of the carrier phase when the frequency offset is a priori known. Note from (15-16) that $1/J_{11}$

depends on the number (N_p) of PS and the number (N_d) of DS, but not on the specific position of the PS in the burst. The bound (20) achieves its *maximum* value at k = - sign(k_G).K, i.e. at one of the edges of the burst interval I (or at both edges if k_G = 0). The difference between the minimum and the maximum value of (20) over the burst amounts to $\Delta^2 4\pi^2 CRB_{FT}$, where $\Delta = K+|k_G|$ represents the distance (in symbols intervals) between the positions of the minimum and maximum value of the CRB (20). Hence, for given values of $1/J_{11}$ and CRB_{FT}^{PS-DS}, the detection of symbols located near the edge k = - sign(k_G).K suffers from a larger instantaneous phase error variance as Δ increases.

Let us define by $\mathbf{J}_\infty$ and $\mathbf{J}_0$ the high-SNR and low-SNR asymptotic FIM, that are obtained as the limit of the FIM for $E_s/N_0 \to \infty$ and $E_s/N_0 \to 0$, respectively. It can be verified that $\mathbf{J}_0$ equals the FIM for estimation from the PS only, that has been shown in [3] to be given by (15) in which the summation over I is replaced with a summation over I_p only. The high SNR asymptotic FIM $\mathbf{J}_\infty$ equals the MFIM from (11) that has been shown to coincide with the high-SNR limit of the FIM for estimation from L random DS in [10]. This indicates that at very high (very low) SNR NDA (DA) estimation techniques may perform close to optimal.

Numerical results were obtained for a QPSK constellation. We assume a burst of L = 321 symbols, containing two parts of $N_p/2$ PS spaced with s DS, as proposed in [11]. Two different burst structures are considered. They are shown in Fig. 1, where the shaded areas indicate the location of the PS. In burst structure #1 the PS are concentrated at the beginning of each burst, whereas burst structure #2 is symmetric yielding k_G = 0, so that carrier phase and frequency estimation are decoupled. We assume that N_p is an even integer and s is an odd integer, or N_p is an odd integer and s equals zero. Figs. 2 and 3 show the ratio CRB^{PS-DS}/MCRB as a function of the SNR, for the reference phase error in k = k_G and for the frequency error. Results are presented for N_p/L equal to (approximately) 10% and 20%, and for several values of s (N_p = 32, 64 if s ≠ 0 and N_p = 33, 65 if s = 0). The $CRB_{DS}(L) = CRB_{PS-DS}(0,L)$ is also displayed. The following observations can be made

- In Fig. 2, the curves for all burst structures with the same ratio N_p/L coincide, as $1/J_{11}$ does not depend on the specific location of the PS in the burst.
- At very low SNR, the bounds become close to their low SNR asymptote that is given by

$$CRB_{\theta_{k_G}}^{PS} = \frac{N_0}{2N_p E_s} \quad (21)$$

$$CRB_{FT}^{PS} = \frac{3N_0}{2\pi^2 E_s [N_p({N_p}^2 - 1) + 3N_p s(s + N_p)]} \quad (22)$$

This low SNR asymptote is a fundamental lower bound on the performance of any DA estimator operating on the known PS only. In a multi-stage synchronization procedure with an initial DA step (see next section) this bound provides an indication of the estimation accuracy after the first stage. Increasing the number of PS decreases both $CRB_{\theta_{k_G}}^{PS}$ from (21) and CRB_{FT}^{PS} from (22). In contrast with $CRB_{\theta_{k_G}}^{PS}$, CRB_{FT}^{PS} depends on the specific position of the PS in the burst. Spreading the PS further across the burst decreases the CRB_{FT}^{PS}. Indeed, for a fixed number of PS N_p, Fig. 3 predicts a better DA frequency estimation performance as the spacing s increases. For fixed N_p and fixed s, the low SNR asymptote of CRB_{FT} is the same for burst structures #1 and #2, as (22) does not depend on the specific position of the pilot sequence within the burst.

- For values of SNR larger than about 10 dB, the bounds become close to their high SNR asymptote, i.e., the MCRB. It has been observed in [12] that CRB_{DS} reaches the MCRB at a value of E_s/N_0 that yields a symbol error rate (SER) of about 10^{-3} (assuming perfect synchronization). We did verify that an SNR of 10 dB corresponds to an SER of about 10^{-3}. Hence, the observation from [12] also holds for the CRBs that take pilot symbols into account.
- For a fixed N_p and fixed s, burst structures #1 and #2 yield the same $CRB_{\theta_{k_G}}$, while the asymmetric burst structure #1 yields the smallest CRB_{FT} (at any SNR). However, as the following example illustrates, we should be very careful when interpreting these results. Fig. 4 depicts the $CRB_{\theta_k}^{PS-DS}$ for the reference phase error as a function of the symbol index k at E_s/N_0 = 2 dB for burst structures #1 and #2 with N_p = 64 and s = 33. The following observations can be made
  - Although burst structure #1 yields the smallest CRB_{FT}, its CRB on the reference phase error variance at k=K is larger than for burst structure #2. This can be explained by noting that, at a value of SNR as low as 2dB, the distance (Δ) between the positions of the minimum and maximum value of the $CRB_{\theta_k}^{PS-DS}$ is significantly larger for burst structure #1 than for burst structure #2.
  - Although burst structure #2 results in the smallest maximum for CRB_{θ_k} over the burst, other than for burst structure #1, this maximum value is reached near both edges of the burst interval. This implies that in burst structure #2 more symbols are affected by a large instantaneous phase error variance than in burst structure #1.

Hence, the 'best' burst structure depends strongly on the operating SNR and on the maximum allowable phase error variance for proper symbol detection.

• $CRB_{PS\text{-}DS}(N_p,N_d)$ is smaller than both $CRB_{PS}(N_p)$ and $CRB_{DS}(N_p+N_d)$. This indicates that it is potentially more accurate to estimate the carrier phase and frequency from a hybrid burst than from a burst without PS or from a limited number of PS only. The ratios $CRB_{DS}(N_p+N_d)/CRB_{PS\text{-}DS}(N_p,N_d)$ and $CRB_{DS}(N_p)/CRB_{PS\text{-}DS}(N_p,N_d)$ depend on the operating SNR and on the burst structure, and indicate to what extent synchronizer performance can be improved by making clever use of the knowledge about the PS and of the presence of the DS in the estimation process.

IV. Practical Estimator Performance

The general maximum likelihood (ML) estimator is known to be asymptotically optimal in the sense that it achieves the performance predicted by the CRB for large data records. However, the performance for finite signal durations cannot be determined analytically. In this section the simulated mean square estimated error (MSEE) of practical joint carrier phase and frequency estimators is compared to the CRB.

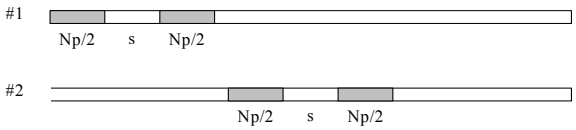

Fig. 1: burst structure, location of the PS

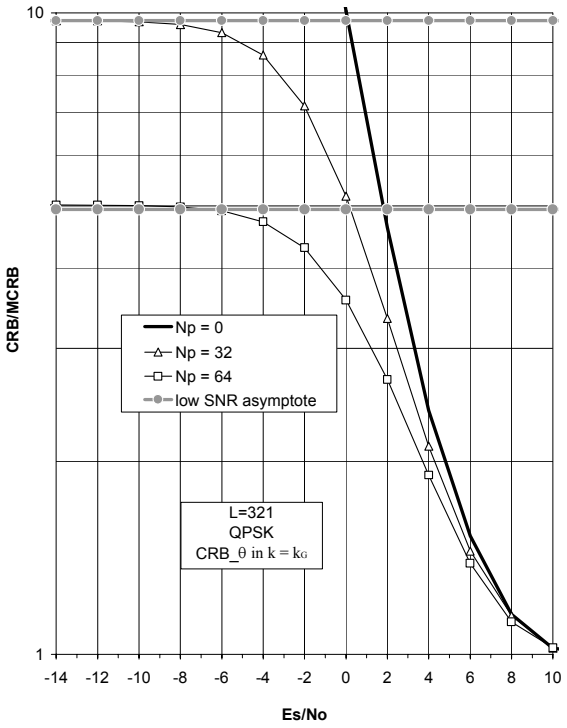

Fig. 2: CRB/MCRB for the reference phase estimate in $k = k_G$

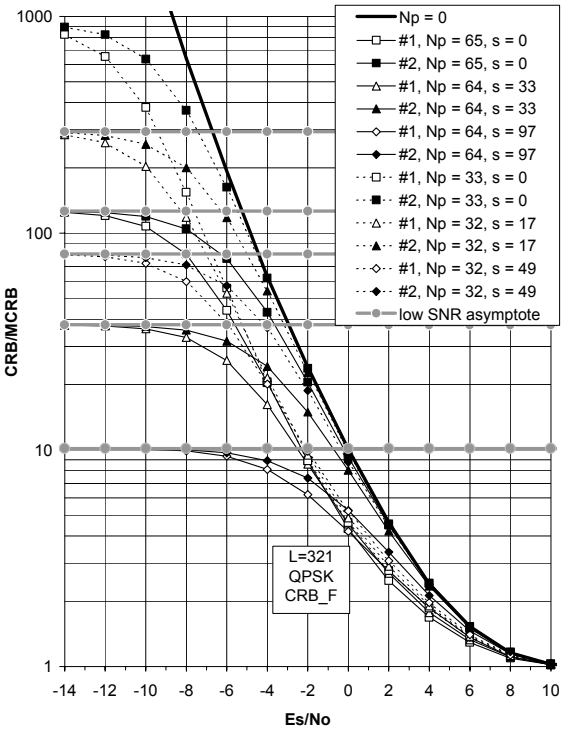

Fig. 3: CRB/MCRB for the frequency estimate

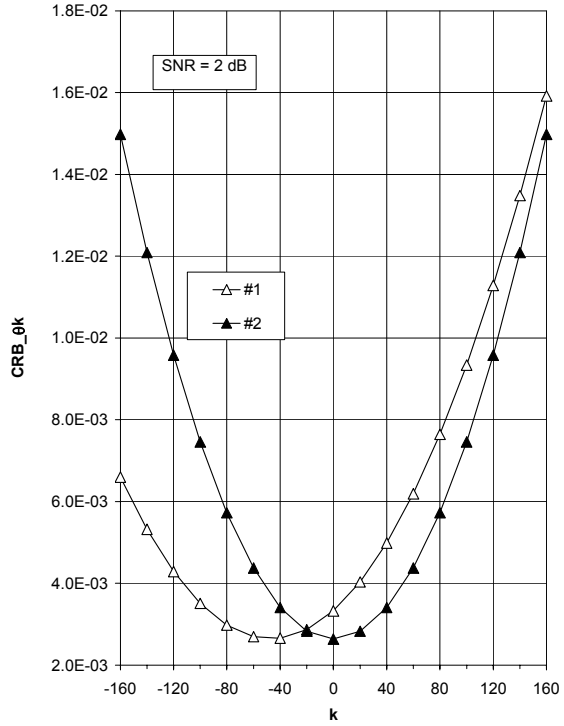

Fig. 4: CRB for the reference phase estimate at $E_s/N_0 = 2dB$

A. DA synchronization

The DA estimates using only the N_p PS are given by

$$\hat{F} = \arg\max_{\tilde{F}} \left(\left| \sum_{k \in I_p} a_k^* r_k e^{-j2\pi k \tilde{F} T} \right| \right) \qquad (23)$$

$$\hat{\theta} = \arg\left\{ \sum_{k \in I_p} a_k^* r_k e^{-j2\pi k \hat{F} T} \right\} \qquad (24)$$

Again, we consider the burst structures from Fig. 1, with L = 321 and QPSK symbols. For several numbers (N_p) of PS and several spacing values (s) , Figs. 5 and 6 show the MSEE of the reference phase estimate in k = k_G and of the frequency estimate. The reference phase error was measured modulo 2π, i.e., in the interval [-π, π]. The DA estimates $\hat{F}$ and $\hat{\theta}_{k_G} = \hat{\theta} + 2\pi k_G \hat{F} T$, resulting from (23) and (24), do not depend on the position of the pilot sequence within the burst. This implies that, for a given value of N_p and s, the corresponding MSEEs are the same for burst structures #1 and #2. At high SNR, the $CRB_{PS}(N_p)$ from (21-22) is reached. Below a certain SNR threshold, the performance dramatically degrades across a narrow SNR interval, with an MSEE much larger than the CRB. This so-called *threshold phenomenon* results from the occurrence of estimates with large errors, i.e., outlier estimates [2]. The presence of important secondary peaks in the likelihood function results in a large probability of generating outlier frequency estimates at lower SNR, because these secondary peaks can more easily exceed the central peak when noise is added. The SNR threshold decreases with the number of available signal samples N_p. For N_p consecutive PS (as in burst structure #1), the threshold is very low so that the DA estimator usually operates above threshold. However, the SNR threshold tends to increase as the PS are separated by DS [3,11]. Fig. 6 shows that s ≈ $N_p/2$ provides a good compromise between a small value of CRB_{FT}^{PS} and a small SNR threshold.

B. NDA synchronization

Assuming a QPSK constellation, the NDA estimates are given by [2,13]

$$\hat{F} = \frac{1}{M} \arg\max_{\tilde{F}} \left| \sum_{k=-K}^{K} |r_k|^2 e^{j4\arg\{r_k\}} e^{-j2\pi k \tilde{F} T} \right| \qquad (25)$$

$$\hat{\theta} = \frac{1}{M} \arg\left\{ \sum_{k=-K}^{K} |r_k|^2 e^{j4\arg\{r_k\}} e^{-j8\pi k \hat{F} T} \right\} \qquad (26)$$

The resulting MSEE converges to $CRB_{DS}(L)$ at high SNR. Simulation results indicate, however, that the value of SNR at which the MSEE becomes close to the CRB may be quite large. The SNR threshold for the NDA estimator is much higher than for the DA estimator, as the non-linearity increases the noise level. To cope with this problem, a two-stage coarse-fine DA-NDA estimator has been proposed in [11]. A ML DA estimator is used to coarsely locate the frequency offset, and then the more accurate NDA estimator attempts to improve the estimate within the uncertainty of the coarse estimator.

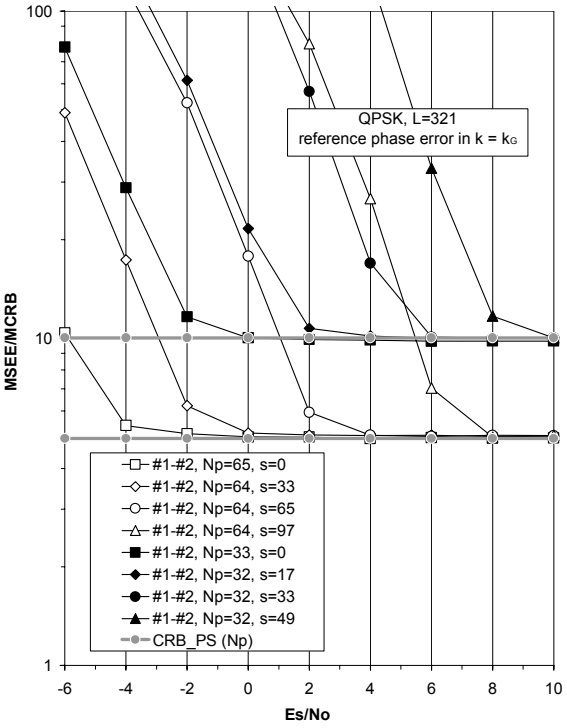

Fig. 5: MSEE/MCRB for the DA ref. phase estimate in k = k_G

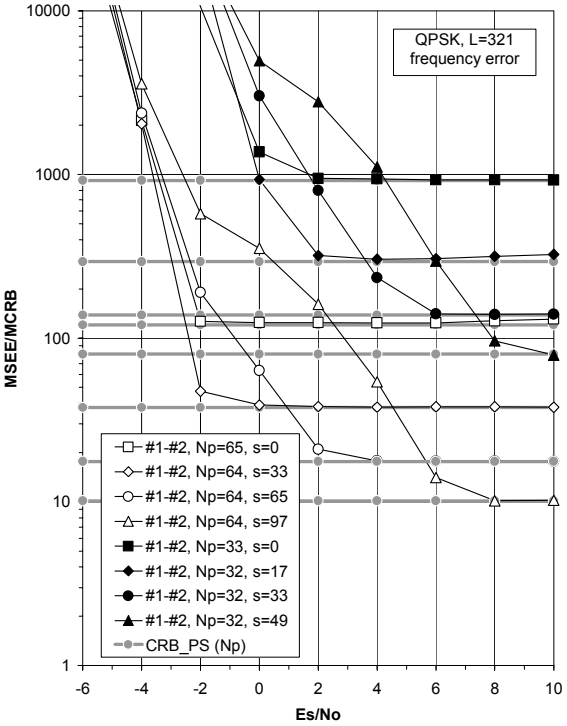

Fig. 6: MSEE/MCRB for the DA frequency estimate

In fact, the search range of the NDA estimator is restricted to the neighborhood of the peak of the DA based likelihood function. This excludes a large percentage of secondary peaks from the search range of the NDA estimator, and thus considerably reduces the probability to estimate an outlier frequency. Assuming the MSEE of the initial DA estimate equals

the $CRB_{FT}^{PS}(N_p)$, this uncertainty range can be determined as $\pm m\sqrt{CRB_{FT}^{PS}(N_p)}$, where m should be carefully chosen. When the parameter m increases, the search region increases, as well as the probability of comprising outlier peaks, which may result in a degradation of the performance *at low SNR* (outlier effect). However, if m decreases, the search region decreases, as well as the probability of comprising the (correct) central peak, which in turn may result in a degradation of the performance *at high SNR*. After frequency and phase correction, the samples for $k \in I_p$ are compared to the original PS and, if necessary, an extra multiple of π/2 is compensated for. A major disadvantage of this DA-NDA algorithm is that it does not exploit the knowledge of the PS in the NDA fine estimation step. Therefore, its MSEE is lower bounded by the $CRB_{DS}(N_p+N_d)$ (with $CRB_{DS}(N_p+N_d) \geq CRB_{PS\text{-}DS}(N_p,N_d)$). This implies that the DA-NDA algorithm is intrinsically suboptimal in the sense that under no circumstances its performance may meet the $CRB_{PS\text{-}DS}$. Some other estimator may yield a MSEE between CRB_{DS} and $CRB_{PS\text{-}DS}$, but it should fully exploit the knowledge of the PS.

C. *Iterative DD synchronization*

DD estimators extend the sum over I_p in (23-24) with terms over I_d in which the quantities a_k are replaced by hard (hDD) or soft (sDD) decisions, that are based upon a previous estimate of (θ, F). For QPSK, the soft decisions are given by [4]

$$\hat{a}_k = \frac{\sinh\left[\frac{2E_s}{N_0}\mathrm{Re}(\tilde{r}_k^{(n-1)})\right] + j\sinh\left[\frac{2E_s}{N_0}\mathrm{Im}(\tilde{r}_k^{(n-1)})\right]}{\cosh\left[\frac{2E_s}{N_0}\mathrm{Re}(\tilde{r}_k^{(n-1)})\right] + \cosh\left[\frac{2E_s}{N_0}\mathrm{Im}(\tilde{r}_k^{(n-1)})\right]} \quad (27)$$

In (27), $\tilde{r}_k^{(n-1)} = r_k e^{-j(\hat{\theta}^{(n-1)} + 2\pi k \hat{F}^{(n-1)}T)}$. The normal operating SNR of the DD estimators is situated above threshold. The required initial estimate $(\hat{\theta}^{(0)}, \hat{F}^{(0)})$ can be obtained from the NDA method; however, the performance below the NDA threshold rapidly degrades, because of an inaccurate initial estimate. If PS are available, it is better to use DA or combined DA-NDA initialization. We will further refer to these schemes as DA-hDD, DA-sDD, DA-NDA-hDD and DA-NDA-sDD. After phase and frequency correction, the samples for $k \in I_p$ are compared to the original PS and, if necessary, an extra multiple of π/2 is compensated for.

Numerical results pertaining to the different algorithms are obtained for a QPSK constellation. We assume a burst with L = 321. The PS are organized as in burst structure #2 from Fig. 1 with N_p = 64 and s = 33. Note that F and θ are decoupled (with $\theta_{k_G} = \theta$). In Figs. 7-8, we have plotted the ratio MSEE/MCRB for

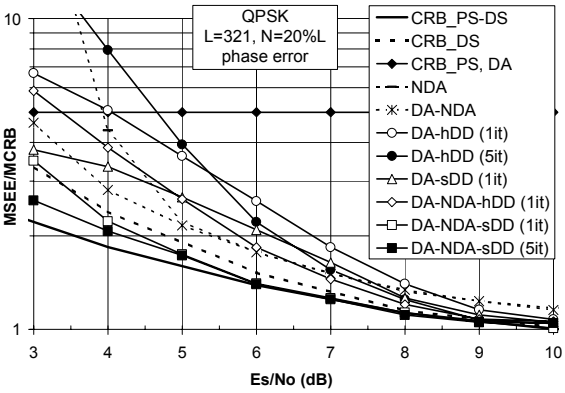

Fig.7: MSEE of the phase estimate

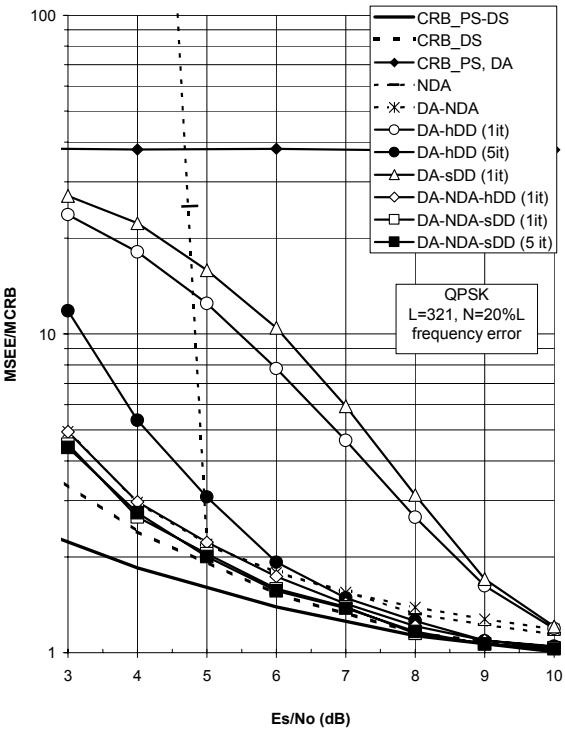

Fig. 8: MSEE of the frequency estimate

the estimation of F and θ as a function of the SNR. The phase error is measured modulo 2π and supported in the interval [-π, π], except for the NDA estimator. The phase error of the NDA estimator was estimated modulo π/2, i.e. in the interval [-π/4, π/4], as this estimator gives a 4-fold phase ambiguity. For the DA-NDA estimation we chose m=3. Our results show that:

- Over the whole SNR range from Figs 7-8, the DA estimator achieves optimal $CRB_{PS}(N_p)$ performance, which is considerably worse than the performance of the hybrid estimators.
- Above its SNR threshold (at about 5dB), the NDA estimator performs very closely to the $CRB_{DS}(L)$.
- At high SNR, the performance of the DA-NDA estimator matches that of the NDA estimator, but the performance below the SNR threshold degrades less rapidly and is still adequate for reliable receiver operation.
- The MSEE resulting from the DA-hDD and DA-NDA-hDD estimators reaches a steady state after

about five iterations. Only at high SNR these estimators outperform the DA-NDA estimator. At (very) low SNR, the performance gets worse when the iteration number increases. This can be seen in Fig. 7 when comparing the DA-hDD after 1 and 5 iterations; the same occurs for the DA-NDA-hDD algorithm (curves not shown). This unexpected behavior indicates that at low SNR the initial estimates are more accurate than the steady-state hDD estimates. Hence, hard decisions are not useful at low SNR.

- The MSEE resulting from the DA-sDD estimator reaches a steady state after 10 to 20 iterations. The DA-NDA-sDD estimator yields the same steady state performance as the DA-sDD estimator, but after considerably less (no more than 5) iterations. This indicates the importance of an accurate initial estimate to speed up convergence. Because these estimators fully exploit PS information, their estimation variance must be compared with CRB_{PS-DS}. The steady state phase MSEE of the DA-NDA-sDD estimator is located between CRB_{DS} and CRB_{PS-DS}, and attains CRB_{PS-DS} for SNR $\geq$ 6 dB (Fig. 7). The fact that the frequency MSEE stays above the CRB_{DS} is an indication of inefficiency (Fig. 8). The DA(-NDA)-sDD estimators outperform by far the DA(-NDA)-hDD estimators and provide a considerable improvement over the DA-NDA estimator.

V. Conclusions

In this contribution, we have investigated the joint phase and frequency estimation from the observation of a 'hybrid' burst that contains PS as well as DS. We have compared the CRB_{PS-DS} with the performance of new and existing carrier synchronizers. Numerical evaluation of this CRB shows that it is potentially more accurate to estimate carrier phase and frequency from a hybrid burst than from a burst without PS or from a limited number of PS only. We have pointed out that the hybrid DA-NDA estimator proposed in [11] is suboptimal, because it does not fully exploit the knowledge about the PS. Further, we have proposed a new iterative sDD estimator with combined DA/NDA initialization, that outperforms the DA-NDA estimator and operates closely to the CRB_{PS-DS}.

Acknowledgement

This work has been supported by the Interuniversity Attraction Poles Program P5/11 – Belgian State – Federal Office for Scientific, Technical and Cultural Affairs

References

[1] H.L. Van Trees, *Detection, Estimation and Modulation Theory*. New York: Wiley, 1968

[2] D.C, Rife and R.R. Boorstyn, "Single-tone parameter estimation from discrete-time observations," *IEEE Trans. Inf. Theory*, vol. IT-20, No. 5, pp. 591-597, Sept. 1974

[3] J.A. Gansman, J.V. Krogmeier and M.P. Fitz, "Single Frequency Estimation with Non-Uniform Sampling," in *Proc. of the 13th Asilomar Conference on Signals, Systems and Computers*, Pacific Grove, CA, pp.878-882, Nov. 1996

[4] W.G. Cowley, "Phase and frequency estimation for PSK packets: Bounds and algorithms," *IEEE Trans. Commun*., vol. COM-44, pp. 26-28, Jan. 1996

[5] F. Rice, B. Cowley, B. Moran, M. Rice, "Cramer-Rao lower bounds for QAM phase and frequency estimation," *IEEE Trans. Commun*., vol. 49, pp 1582-1591, Sep. 2001

[6] N. Noels, H. Steendam and M. Moeneclaey, "The true Cramer-Rao bound for phase-independent carrier frequency estimation from a PSK signal," in *Proc. IEEE Globecom 2002*, Taipe, Taiwan, paper CTS-04-2, Nov. 2002

[7] N. Noels, H. Steendam and M. Moeneclaey, "The Impact of the Observation Model on the Cramer-Rao Bound for Carrier and Frequency Synchronization", in *Proc. IEEE Int. Conf. Communications 2003*, Anchorage, Alaska, Paper CT04-1, 11-15 May 2003

[8] A.N. D'Andrea, U. Mengali and R. Reggiannini, "The modified Cramer-Rao bound and its applications to synchronization problems," *IEEE Trans. Comm*., vol COM-24, pp. 1391-1399, Feb.,Mar.,Apr. 1994.

[9] F. Gini, R. Reggiannini and U. Mengali, "The modified Cramer-Rao bound in vector parameter estimation," IEEE Trans. Commun., vol. CON-46, pp. 52-60, Jan. 1998

[10] M. Moeneclaey, "On the true and the modified Cramer-Rao bounds for the estimation of a scalar parameter in the presence of nuisance parameters," *IEEE Trans. Commun*., vol. COM-46, pp. 1536-1544, Nov. 1998

[11] B. Beahan and B. Cowley, "Frequency Estimation of Partitioned Reference Symbol Sequences," master thesis supervisor B. Cowley, www.itr.unisa.edu.au/~steven/thesis

[12] N. Noels, H. Steendam and M. Moenecaley, "Carrier Phase recovery in Turbo receivers: Cramer-Rao bound and synchronizer performance," accepted for publication in *Proc. International symposium on turbo coded and related topics (ISTC) 2003*, Brest, France, 31 Aug. -5 Sept. 2003

[13] A.J. Viterbi and A.M. Viterbi, "Nonlinear estimation of PSK-modulated carrier phase with application to burst digital transmission," *IEEE Trans. Inform. Theory*, vol. IT-29, pp. 543-551, July 1983